Perifoveal Cone- and Rod-Mediated Temporal Contrast Sensitivities in Stargardt Disease/Fundus Flavimaculatus

Julien Fars,[1] Francesca Pasutto,[2] Jan Kremers,[1] and Cord Huchzermeyer[1]

[1]Department of Ophthalmology, University Hospital Erlangen, Erlangen, Germany
[2]Institute of Human Genetics, Friedrich-Alexander-Universität Erlangen-Nürnberg, Erlangen, Germany

Correspondence: Cord Huchzermeyer, Department of Ophthalmology, University Hospital Erlangen, Schwabachanlage 6, 91054 Erlangen, Germany;
cord.huchzermeyer@uk-erlangen.de.

PURPOSE. The purpose of this study was to compare L-cone–driven, S-cone–driven, and rod-driven temporal contrast sensitivities (tCSs) in patients with Stargardt disease 1/fundus flavimaculatus (STGD1/FF).

METHODS. Fourteen patients (eight male, six female; mean age, 43.21 ± 13.18 years) with genetically confirmed STGD1/FF participated in this study. A dedicated light-emitting diode stimulator was used to measure perifoveal tCSs in an annular test field ($1°–6°$ of visual eccentricity) at temporal frequencies between 1 and 20 Hz. Photoreceptor classes were isolated with the triple silent substitution technique. To compare functional damage among photoreceptor classes, sensitivity deviations (decibels) were calculated based on age-related normal values and then averaged across those frequencies where perception is mediated by the same post-receptoral pathway (L-cone red–green opponent pathway: 1, 2, 4 Hz; luminance pathway: 12, 16, 20 Hz; S-cone pathway: 1, 2, 4 Hz; fast rod pathway: 8, 10, 12 Hz). Sensitivity deviations were compared with infrared scanning laser ophthalmoscopy (IR-SLO) and standard automated perimetry (SAP).

RESULTS. Photoreceptor-driven tCSs were generally lower in patients with STGD1/FF than in normal subjects but were without systematic differences among photoreceptors. Although sensitivity deviations were significantly correlated between each other, only luminance-driven L-cone sensitivity deviations were significantly correlated with the IR-SLO area of hyporeflectance (AoH) and SAP central mean deviation within $6°$ eccentricity (MD_{6deg}).

CONCLUSIONS. No systematic differences between photoreceptor classes were detected; however, our data suggest that temporal contrasts detected by the luminance pathway were closely correlated with other clinical parameters (AoH and MD_{6deg}) and might be most useful as functional biomarkers in clinical trials.

Keywords: temporal contrast sensitivity, Stargardt disease, fundus flavimaculatus, perifovea, photoreceptors

Stargardt disease 1 (STGD1) and fundus flavimaculatus (FF) are the most frequent, often overlapping phenotypes caused by recessive mutations in the *ABCA4* gene, a transmembrane ATP-binding cassette (ABC) transporter in the photoreceptors.[1,2] STGD1, the leading cause of Mendelian macular dystrophy (MIM 248200), was first described by Karl Stargardt[3] as a juvenile macular dystrophy with a central atrophic lesion surrounded by yellow–white flecks. Sometimes the fovea is spared, so that patients present with a bull's-eye maculopathy (BEM),[4] but foveal sparing may progress to central atrophy. FF (MIM 248200) is characterized by orange–yellow flecks distributed over the posterior pole, either with or without atrophic lesions.[5] Additionally, recessive *ABCA4* mutations also affect the peripheral retina, resulting in generalized cone–rod dystrophy[6] or retinitis pigmentosa.[7]

The central lesions often include atrophy of the retinal pigment epithelium (RPE), which can be characterized by a dark area of absent fundus autofluorescence. However, the area of hyporeflectance in the infrared scanning laser ophthalmoscopy (IR-SLO) images (frequently displayed as an en face image alongside OCT sections) is usually larger than the area of hypofluorescence. It is caused by disruption of the outer retinal layers and shows a strong association with the area of decreased perimetric sensitivity.[8]

Characterization of visual function in STGD1/FF is complex due to the variability of phenotypes. *ABCA4* is expressed in both cones[2] and rods.[2] STGD1/FF may cause not only loss of visual acuity,[9] central or ring-shaped scotomata,[10] and color vision defects,[11] but also impaired dark adaptation.[12] Most functional endpoints, such as visual acuity and microperimetry, progress slowly, which renders them less useful for trials of therapies that halt progression. New functional endpoints are needed, and scotopic, rod-driven microperimetry has been suggested as an alternative.[13,14] Photopic (cone-dominated) and scotopic (rod-dominated) function can progress at different rates in the beginning of peripheral retinal degeneration.[13]

The current techniques for isolated measurements of cone- or rod-mediated retinal function, especially light- and

dark-adapted chromatic perimetry, do not always allow sufficient isolation.[15] In contrast, the silent substitution technique[16,17] enables reliable isolation of responses of photoreceptor subtypes in psychophysical tests[18–20] and electroretinograms (ERGs).[21,22] Importantly, isolation of the responses of the different photoreceptor types can be obtained at equal states of luminance and chromatic adaptation. Thus, when using the triple silent substitution, losses of temporal contrast sensitivity (tCS) can be compared directly among photoreceptor types.[20] We have validated the technique to measure photoreceptor-isolating, perifoveal tCS in normal subjects, dichromats, and an S-cone monochromat.[18,19] In addition, we were able to demonstrate tCS losses in patients with glaucoma and retinitis pigmentosa.[20,23]

In the present study, we measured photoreceptor-isolating tCSs in the perifovea in patients with STGD1/FF with the purpose of (1) determining the feasibility of such measurements, (2) comparing losses in tCS among photoreceptor types, and (3) investigating how these tCS losses relate to established clinical outcome parameters.

METHODS

Subjects

Fourteen patients with STGD1/FF (12 of them genetically confirmed) participated in this study (eight males, six females; ages 24–63 years; mean age, 43.21 ± 13.18 years). All participants gave prior written informed consent. The study adhered to the tenets of the Declaration of Helsinki and was approved by the ethics committee of the Friedrich-Alexander-Universität Erlangen-Nürnberg. Clinical examinations consisted of subjective and objective refraction, best-corrected visual acuity, slit-lamp examination, air-puff tonometry, and dilated funduscopy. Accordingly, patients were subdivided into three groups (fundus flavimaculatus, bull's-eye-maculopathy, and central foveal atrophy [CFA]), which are described in Table 1. This classification is partially based on the fixation locus, which came from the infrared SLO images that were obtained simultaneously with the OCT measurements and validated with the visual field measurements.

Exclusion criteria were the presence of concomitant ocular diseases, especially clinically significant opacification of the optic media, severe refractive errors (myopia, < −8 diopter [D]; hyperoperia, > +4 D; astigmatism, > 2 D), medical therapies that are known to impair visual function, and systemic diseases that might affect visual function.

Genetic Testing

Genomic DNA was prepared from peripheral blood samples by a standard salting-out protocol using the FlexiGene DNA Kit (QIAGEN, Hilden, Germany). Complete coding regions of the *ABCA4* and *OPN1L/OPN1W* genes including flanking intronic/untranslated region sequences were amplified by polymerase chain reaction (PCR) using appropriate amplification protocols. Primer sequences for *ABCA4* were selected using Primer3 software (http://frodo.wi.mit.edu/cgi-bin/primer3/primer3_www.cgi/) and were supplied by Thermo Fisher Scientific (Waltham, MA, USA). *ABCA4* primer sequences are available upon request. Purified PCR fragments were sequenced using BigDye Terminator 3.1 (Applied Biosystems, Waltham, MA, USA) on an automated capillary sequencer (3730 Genetic Analyzer; Applied Biosystems) and analyzed using SeqPilot and Sequencer 5.1 software. GenBank accession number NM_000350.2 was used as the reference sequence for the *ABCA4* gene.

Temporal Contrast Sensitivities

Temporal contrast sensitivities were measured with a two-channel Maxwellian view optical system with four light-emitting diode (LED) primaries in each channel. Technical details[24] and calibration procedures[18] have been described previously. The spectral outputs of the LEDs peaked at 660 nm (red), 558 nm (green), 516 nm (cyan), and 460 nm (blue) and were narrowed to an 8- to 10-nm bandwidth at half-height by interference filters. LED luminances were driven independently by the eight channels of a personal computer soundcard (Xonar D2/PM, ASUSTek, Taipei, Taiwan)[25] based on fourth-order polynomials that were fitted to LED luminances as a function of input strength. The stimuli were viewed through a 3-mm-diameter artificial pupil positioned in the focus (i.e., pupil plane) of the Maxwellian view system close to the subject's pupil. According to our calculations,[18] natural pupil size was always larger than 3 mm at all retinal illuminances that we used, regardless of age. Corrective lenses were added at the pupil plane when necessary (myopia or hyperopia with spherical equivalent > ±1 D). The use of an artificial pupil together with chin and forehead rests was sufficient to stabilize the head and more acceptable than bite bars, especially for elderly patients. Minor head movements were not problematic, and mispositioning could be identified by semilunar shadows at the edge of the test field. Observers were instructed to attain a correct head positioning so that the complete stimulus was visible. They were encouraged to take their time to find a comfortable head position.

The spatial and temporal structure of the stimuli are illustrated in Figure 1. Briefly, the test field had an annular shape with 2° inner and 13° outer diameter projected onto the perifoveal retina. The rationale for choosing this spatial arrangement was to minimize the influence of the macular pigment on the rod and cone fundamentals. In this field, luminances of the four primaries were modulated sinusoidally over time using temporal contrasts that modulated the excitation of

TABLE 1. Groups and Descriptions of the Patients With Stargardt Disease

Group	Description	Fixation	Visual Acuity	Visual Field
FF	Fundus flavimaculatus: yellowish flecks surrounding the macula without any central atrophic lesion	Central	Good	Good
BEM	Bull's-eye maculopathy: ring of retinal atrophy surrounding the fovea	Central	Good	Ring-shaped scotoma
CFA	Central foveal atrophy: ring of flecks surrounding a central, atrophic appearing macular lesion	Eccentric	Poor	Superior scotoma
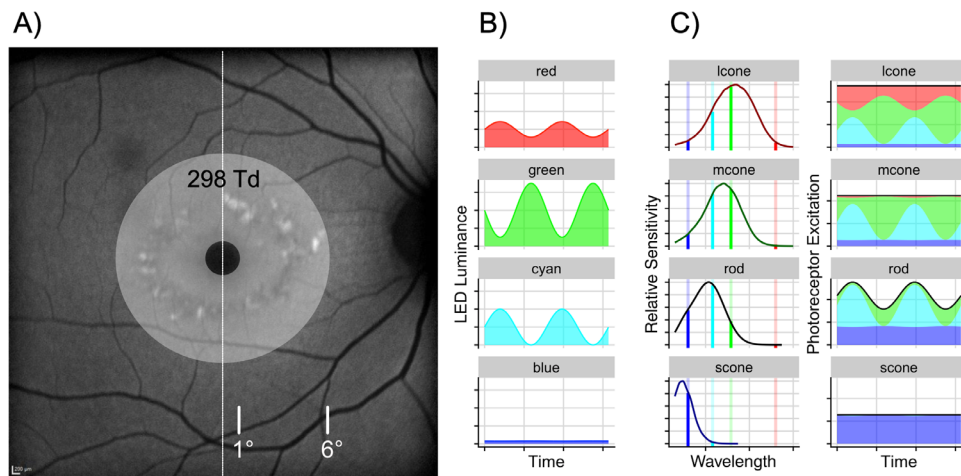
FIGURE 1. Spatial and temporal configuration of the stimuli. (**A**) The perifoveal test field had an inner diameter of 2° and an outer diameter of 12°. The time-averaged stimulus conditions were always 289 phot td with CIE coordinates $x = 0.38$ and $y = 0.28$. (**B**) Example of how the four primaries were temporally modulated sinusoidally around their respective mean luminances in order to create a rod stimulus. (**C**) The spectral sensitivity curves show how the LEDs contributed differently to photoreceptor excitation in the four photoreceptor types. Due to these differences in spectral sensitivities, photoreceptor excitation was modulated in only one photoreceptor type (in this example, rods), whereas luminance changes compensated each other in the remaining three (triple silent substitution).

a single photoreceptor type while the others were silenced (see below). The central circular field of 2° diameter was used as the fixation target. Subjects were requested to fixate the center of this field if they were able to identify it or to look straight ahead, centering a central scotoma in the surround field. The unmodulated center and the modulated annular field had equal time-averaged chromaticities that were close to equal-energy white with coordinates of $x = 0.38$ and $y = 0.28$ in the CIE 1931 chromaticity diagram. The time-averaged retinal illuminance produced by the annular field was 289 photopic trolands (phot td). In the central field, retinal illuminance was set to 144.5 phot td in order to avoid foveal stimulation through stray light.

Rod- and cone-isolating stimuli were created using the triple silent substitution paradigm (Figs. 1B, 1C),[17,26] as described previously.[18] Briefly, successful silent substitution ensures that detection of temporal contrasts is mediated by only one photoreceptor class. Contrasts at photoreceptor level were calculated based on the Stockman and Sharpe 10° cone fundamentals for cones[27,28] and the scotopic luminous efficiency, $V'(\lambda)$, for rods.[29] Photoreceptor contrasts were varied by proportional variation of the LED contrasts so that their contrast ratios and their relative phases remained constant and silent substitution was ensured at all contrasts. The gamut (i.e., maximal possible cone or rod contrasts) of the stimulator was 24.95% L-cone contrast, 22.33% M-cone contrast, 82.75% S-cone contrast, and 27.30% rod contrast.

Detection thresholds were determined at nine different temporal frequencies (1, 2, 4, 6, 8, 10, 12, 16, and 20 Hz) using a modified yes/no Parametric Estimation by Sequential Testing (PEST) procedure, where subjects had to indicate whether or not they perceived a temporal modulation (flicker). We used two randomly interleaved staircases, one starting at 0% and the other one at maximal contrast. The contrast was increased when the subjects did not perceive flicker and decreased when they perceived the modulation. The initial contrast change was 20% of the maximally possible contrast. Contrast step size was halved, and its direction was inversed at each perceptual reversal (from flicker perception to no flicker perception and vice versa). The

termination criterion was either a step size of one-seventh or less of the current contrast after at least two reversals or no flicker perception at maximal possible contrast for three times.

IR-SLO and Optical Coherence Tomography

IR-SLO images and optical coherence tomography (OCT) scans (Fig. 2) were acquired simultaneously with the Heidelberg Retina Analyzer (HRA; Heidelberg Engineering, Heidelberg, Germany). In contrast to the measurements with the LED stimulator, where subjects with central scotoma were asked to center the scotoma in the test field, the subjects were asked to directly fixate the target provided by the HRA in these measurements. This enabled us to estimate the fixation target from these measurements.
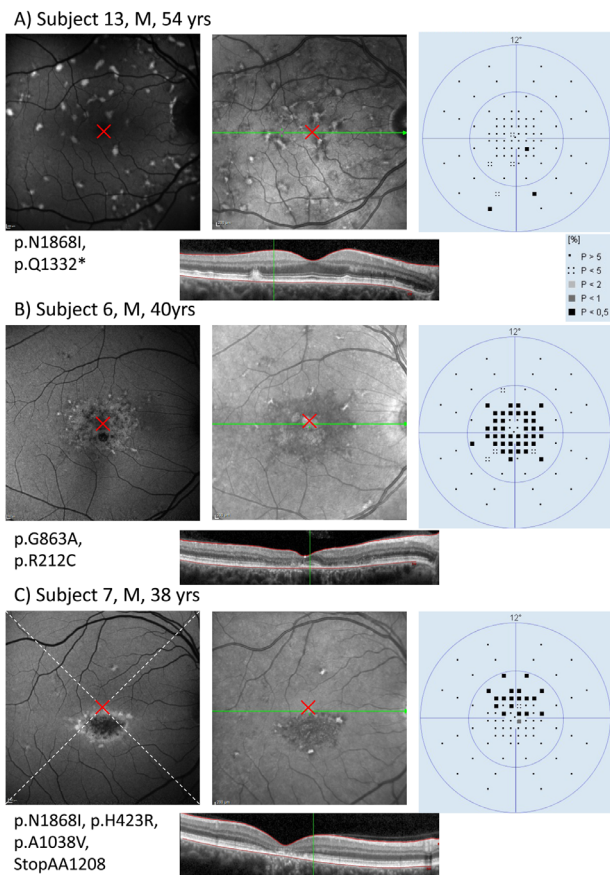
For each patient, the area of hyporeflectance (AoH) was measured using the area tool of the Heidelberg Eye Explorer software on the IR-SLO images. When detection of the border was difficult in these images, OCT scans were used to facilitate identification. In subjects with BEM, the central unaffected area was subtracted from the AoH. In patients with pure fundus flavimaculatus (without foveal atrophy), AoH was considered to be zero.

Visual Fields

Standard automated perimetry was performed using the Octopus 900 perimeter (Haag-Streit, Köniz, Switzerland). Subjects were asked to directly fixate the small central light provided by the Octopus 900. As a consequence, most patients with STGD1 with CFA had scotomata above the point of fixation.

We used the M pattern, which consists of 81 locations within the central 10° of the visual fields. Visual fields were exported and analyzed with the visualFields package of the R programming language (R Foundation for Statistical Computing, Vienna, Austria).[30] Mean deviations (MD_{6deg}) were calculated manually by averaging defect values from all locations between 1° to 6° of radius eccentricity.

A) Subject 13, M, 54 yrs

p.N1868I,
p.Q1332*

B) Subject 6, M, 40yrs

p.G863A,
p.R212C

C) Subject 7, M, 38 yrs


p.N1868I, p.H423R,
p.A1038V,
StopAA1208

FIGURE 2. IR-SLO (*left*), OCT (*middle*), and standard automated perimetry (*right*) from three patients who were representative of the three groups. (**A**) Data from a subject with FF; (**B**) data from a subject with BEM; and (**C**) data from a subject with CFA. The *red crosses* show the fixation loci, and the *dashed white lines* show that these are located in the center of the OCT image. Note that the OCT scan shows the foveola; therefore, the OCT in (**C**) does not correspond to the *green line* in the infrared SLO scan right above.

Data Analysis

Data analysis was conducted using R. The tCS values were defined as 100 times the inverse of the photoreceptor contrast at threshold (in percent). The temporal contrast sensitivity functions (tCSFs) show contrast sensitivity as a function of the temporal frequency.

For comparison among photoreceptors, we calculated sensitivity deviation values (dB) as the difference between age-adjusted log sensitivity values of the patients and the normal log sensitivities (1 dB = 0.1 log contrast sensitivity). Age adjustment was based on previously described measurements.[20] A negative sensitivity deviation corresponded to a loss of function. To reduce the number of statistical comparisons, we calculated a mean deviation (MD) by averaging sensitivity deviations over a range of frequencies where detection is expected to be mediated by a single retinogeniculate pathway and without intrusion by other pathways[18,19,31]: (1) LMD_{low}, red–green opponent pathway-mediated L-cone–driven sensitivities at 1, 2, and 4 Hz; (2) LMD_{high}, luminance pathway-mediated L-cone–driven sensitivities at 12, 16, and 20 Hz; (3) SMD, blue–yellow opponent pathway-mediated S-cone–driven sensitivities at 1, 2, and 4 Hz; and (4) RMD, rod-driven sensitivities at 8, 10, and
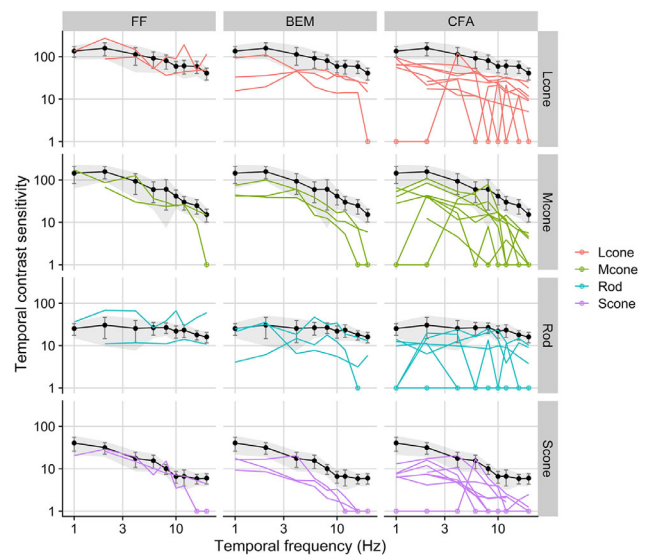
FIGURE 3. Age-adjusted tCSFs of the four photoreceptor types (L-, M-, and S-cones and rods) in 13 patients from the three patient groups. Reference values[20] are shown in *black*. The *error bars* and the *shaded gray areas* indicate confidence intervals for the normal values and ±1 SD, respectively. TCSs in the FF group were close to normal. Patients with BEM had reduced tCSs. The reduction was even larger for patients with CFA. Floor effects, where patients were unable to see the maximally achievable contrast, are represented by the *open crossed circles* (tCS set to 1.0).

12 Hz. L-cone and M-cone sensitivity deviations were found to be highly correlated (indicating that the same pathways were involved). We therefore only used L-cone stimuli for measuring deviations in parvo- and magnocellular pathway-mediated sensitivities.

We used the Mann–Whitney *U* test for identifying statistically significant differences in sensitivity deviation between patients and normal subjects. The differences among patient groups were tested using Kruskall–Wallis tests followed by Dunn's test with Bonferroni correction for multiple testing. The significance of correlations between clinical features was assessed with Pearson correlation coefficients, multiple testing was corrected using Holm's correction. Significance level for all tests was set at $P < 0.05$.

When patients were unable to perceive the highest contrast technically possible for the given photoreceptor type (LED stimulator gamut), we proceeded depending on the type of analysis. For the tCSFs we used a sensitivity of 1.0 as an estimate when such floor effects occurred (Figs. 3 and 4), and for the sensitivity loss plots we age-adjusted the sensitivity that corresponded to a threshold exactly at the gamut of the device as a more conservative estimate instead (Fig. 5). However, this leads to lower sensitivity loss estimates at higher ages, because normal values decrease with age; therefore, we did not include these estimates in the calculation of mean deviations.

Results

Clinical and demographic patient characteristics are shown in Table 2. Clinical findings of three patients that are representative of the three diagnosis groups are displayed in Figure 2. *ABCA* sequence variants of the 14 patients who were genetically screened are shown in Table 3. Two
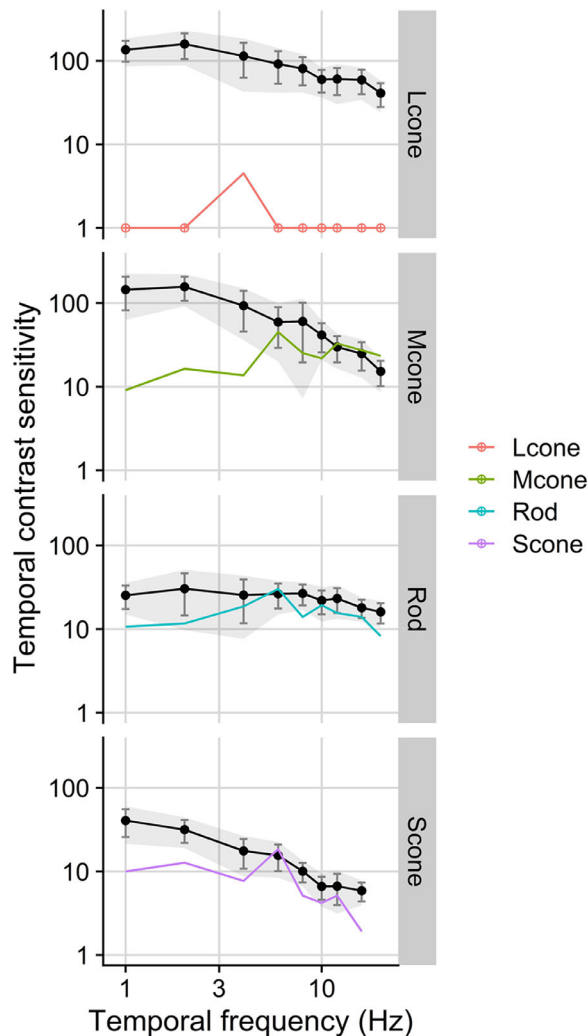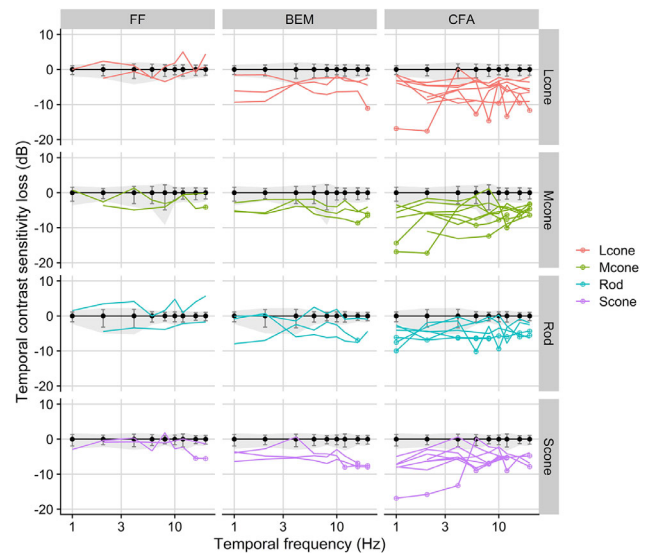
FIGURE 4. Patient 9's temporal contrast sensitivity functions. L-cone, M-cone, rod, and S-cone sensitivities are represented in *red, green, blue,* and *purple,* respectively. Reference values[20] are shown in black. The *error bars* and the *shaded gray areas* indicate confidence intervals for the normal values and ±1 SD, respectively. Floor effects, where patients were unable to see the maximally achievable contrast, are represented by the *open crossed circles* (tCS set to 1.0).

FIGURE 5. Age-adjusted tCSFs losses relative to normal data of the four photoreceptor types (L-, M-, and S-cones and rods) in 13 patients from the three patient groups. The *error bars* and the *shaded gray areas* represent the confidence intervals and ±1 SD. The losses were largest in the CFA group, the BEM group displayed mild losses, and the FF group was close to normal. Losses were calculated by using the maximal technically achievable contrast for this photoreceptor type as a conservative estimate for the threshold and subtracting this from the age-adjusted normal values.[20] These estimates are shown as circles with crosses.

patients had FF but neither foveal atrophy nor other abnormalities of the neurosensory retina in the OCT scans. These patients had good visual acuities. One patient had a normal visual field, and the other one had a slightly subnormal visual field (MD_{6deg} of −0.6 dB and −3.2 dB, respectively).

BEM was found in three patients. These patients had good visual acuities but characteristic visual field defects (MD_{6deg} of −15.6 dB, −5.29 dB, and −8.4 dB). Patients from both groups (FF and BEM) fixated centrally.

CFA and eccentric fixation were present in the remaining nine patients. In Patient 8, OCT changes were more pronounced in the perifovea than in the foveola, suggesting that this patient had lost central fixation and converted from BEM to CFA relatively recently.[32] Furthermore, this patient did not have a well-defined area of pigment epithelial atrophy, but a relatively large AoH (8.2 mm²). All patients in the CFA group had retinal fixation loci at the upper edge of the area of hypofluorescence in the IR-SLO. Consequently, scotomata were in the upper hemisphere of the visual fields.

A female patient (Patient 9) from this group was not included in the analyses of L-cone or M-cone responses, because she had highly abnormal photoreceptor-specific temporal contrast sensitivities that were indicative of protanopy. This was confirmed by subsequent anomaloscopy and genetic testing of *OPN1L/OPN1W*. Her results are reported separately below.

LED Stimulator tCSFs and Loss Functions

The age-adjusted tCSFs for 13 of the 14 patients are shown in Figure 3. The shapes of the tCS curves were largely similar to those of normal subjects, indicating that perception was mediated by the same retinogeniculate pathways. The patients with FF had values close to normal. BEM and CFA patients had markedly reduced tCSs. In the CFA group, floor effects were frequently present, and some patients had large differences in tCS between adjacent frequencies, possibly caused by unstable fixation.

Patient 9 was not included in the analysis of L-cone–driven and M-cone–driven tCS, because her tCSF revealed characteristic features of protanopy, as described in an earlier study (shown in Fig. 4).[18] L-cone sensitivities were minimal over the entire frequency range. M-cone sensitivities were reduced at low temporal frequencies, indicating a dysfunctional red–green opponent system.[18] This color vision deficiency was confirmed by the anomaloscope results (Rayleigh equation) and by demonstrating sequence variants of the opsin genes (amino acid sites 116: Ser/Tyr; 180: Ser/Ala; 230: Ile/Thr), indicating that only M-cone pigment was expressed.

The age-adjusted sensitivity losses of the 13 patients are presented in Figure 5. As a conservative estimate, the age-adjusted gamut of the device was used to calculate the

Table 2. Demographic and Clinical Characteristics of Patients

ID	Age (y)	Gender	Eye	Classification	LogMAR	Hyporeflectance Area (mm^2)	6° Perimetric Mean Deviation (dB)
1	62	Male	R	Central foveal atrophy	0.884	—	—
2	31	Female	R	Central foveal atrophy	1.398	4.76	−27.763
3	54	Male	R	Fundus flavimaculatus	0.5	0	−3.248
4	27	Female	R	Central foveal atrophy	0.9	6.18	−2.517
5	24	Female	R	Central foveal atrophy	0.9	3.93	−14.846
6	40	Male	R	Bull's-eye maculopathy	0.1	7.99	−15.598
7	38	Male	R	Central foveal atrophy	0.7	3.2	−9.304
8	49	Male	R	Central foveal atrophy	0.5	8.2	−10.517
9*	38	Female	L	Central foveal atrophy	0.823	4.16	−4.354
10	63	Female	L	Central foveal atrophy	0.519	3.9	−10.377
11	61	Male	R	Central foveal atrophy	0.4	6.39	−12.317
12	34	Female	R	Bull's-eye maculopathy	0.027	5.29	−2.673
13	54	Male	R	Fundus flavimaculatus	0.147	0	−0.635
14	30	Male	R	Bull's-eye maculopathy	−0.009	3.4	−8.407

Patient 9 was not included in the analyses of L-cone–driven sensitivities because of findings that were indicative of protanopy (see text).

Table 3. Genetic Characterization of Patients

ID	Age (y)	Allele	Protein	dbSNP	gnomAD	Clinical Interpretation
1	62	—	—	—	—	—
2	32	—	—	—	—	—
3	54	c.1937+1G>A		rs61752401	0.00003	Pathogenic
4	27	c.746A>G	p.(Asp249Gly)	rs62646865		Uncertain significance
		c.6320G>A	p.(Arg2107His)	rs62642564	0.00203	Conflicting
		c.5693G>A	p.(Asn1868Ile)	rs1801466	0.04255	Conflicting
		c.6764G>T	p.(Ser2255Ile)	rs6666652	0.07149	Benign
5	24	c.5882G>A	p.(Gly1961Glu)	rs1800553	0.00456	Conflicting
		MLPA: DelEx21-22-23	—	—	—	—
6	40	c.634C>T	p.(Arg212Cys)	rs61750200	0.00006	Pathogenic
		c.2588G>C	p.(Gly863Ala)	rs76157638	0.00376	Likely pathogenic
7	38	c.3113C>T	p.(Ala1038Val)	rs61751374	—	Pathogenic
		c.3617delA	p.(Asn1206Metfs*3)	—	—	Pathogenic
		c.5603A>T	p.(Asn1868Ile)	rs1801466	0.04255	Conflicting
		c.1268A>G	p.(His423Arg)	rs3112831	0.26037	Benign/likely benign
8	49	c.967delC	p.(Leu323Cysfs*51)	—	—	Pathogenic
		c.1268A>G	p.(His423Arg)	rs3112831	0.26037	Benign/likely benign
		c.2828G>A	p.(Arg943Gln)	rs1801581	0.02951	Benign/likely benign
		c.5882G>A	p.(Gly1961Glu)	rs1800553	0.00456	Conflicting
9	38	c.1268A>G	p.(His423Arg)	rs3112831	0.26037	Benign/likely benign
		c.5311G>A	p.(Gly1771Arg)	rs374015407	0.000004	—
		c.5882G>A	p.(Gly1961Glu)	rs1800553	0.00456	Conflicting
10	63	c.6282+7G>A	—	rs17110761	0.08189	Benign
		c.6764G>T	p.(Ser2255Ile)	rs6666652	0.07149	Benign
11	61	c.1411G>A	p.(Glu471Lys)	rs1800548	0.00083	Uncertain significance
		c.1903C>T	p.(Gln635*)	rs61749414	—	Pathogenic
		c.5603A>T	p.(Asn1868Ile)	rs1801466	0.04255	Conflicting
12	34	c.2565_2572del	p.(Trp855*)	—	—	Pathogenic
		c.5603A>T	p.(Asn1868Ile)	rs1801466	0.04255	Conflicting
13	54	c.3994C>T	p.(Gln1332*)	—	—	Pathogenic
		c.5603A>T	p.(Asn1868Ile)	rs1801466	0.04255	Conflicting
14	30	c.1937+1G>A	—	rs61752401	0.00003	Pathogenic
		c.5603A>T	p.(Asn1868Ile)	rs1801466	0.04255	Conflicting

dbSNP, Single Nucleotide Polymorphism Database; gnomAD, Genome Aggregation Database; Conflicting, conflicting interpretation of pathogenicity.

loss when the patients were not able to detect the largest contrast. In general, no clear frequency-dependent losses were observed except in one patient with CFA; however, this patient's responses were variable at low frequencies.

tCS Mean Deviations

Figure 6 and Table 4 compare photoreceptor-specific tCS mean deviations for different photoreceptor types and post-receptoral pathways. The individual data points are
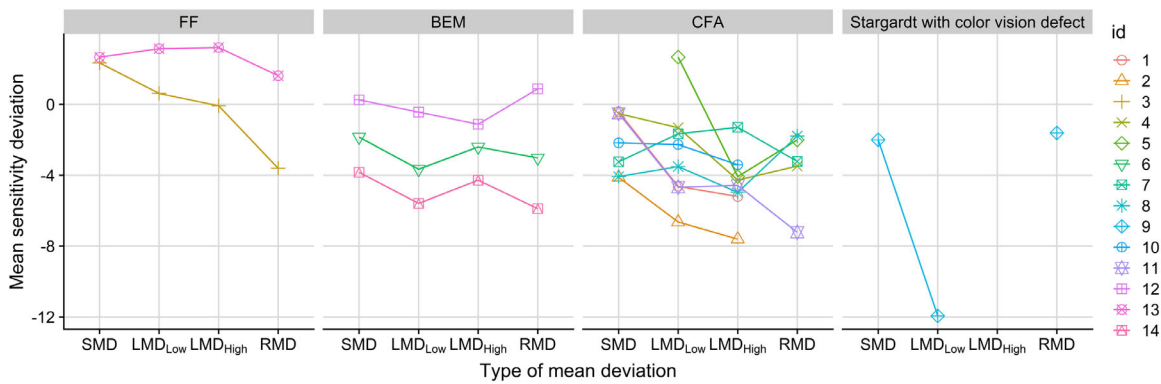
FIGURE 6. Slope plots show differences between the mean sensitivity deviations of the different photoreceptor types and/or post-receptoral pathways in the three patient groups and in Patient 9 (STGD with protanopic color vision defect). The connecting lines do not indicate interpolation between measured values but facilitate intraindividual comparisons among photoreceptor types. The fact that most lines are not steep indicates generalized rather than photoreceptor-specific loss of function, but there seemed to be a tendency toward lower LMD$_{High}$ values in the CFA group.

TABLE 4. Temporal Contrast Sensitivity Mean Deviations

ID	Age (y)	Gender	Eye	LMD$_{Low}$ (dB)	LMD$_{High}$ (dB)	SMD (dB)	RMD (dB)
1	62	Male	R	−4.637	−4.939	−0.41	—
2	31	Female	R	−6.598	−7.487	−3.662	—
3	54	Male	R	0.624	−0.075	2.368	−3.526
4	27	Female	R	−1.194	−4.137	−0.507	−3.396
5	24	Female	R	2.659	−4.093	—	−1.935
6	40	Male	R	−3.565	−2.408	−1.85	−2.844
7	38	Male	R	−1.35	−1.248	−3.12	−3.161
8	49	Male	R	−3.083	−4.896	−3.816	−1.361
9	38	Female	L	−11.848	—	−1.855	−1.516
10	63	Female	L	−2.209	−3.384	−2.115	—
11	61	Male	R	−4.147	−4.547	−0.276	−7.223
12	34	Female	R	−0.409	−1.044	0.459	0.873
13	54	Male	R	3.218	3.351	2.758	1.615
14	30	Male	R	−5.596	−3.838	−4.279	−5.887

LMD$_{Low}$, mean deviations for L-cones at low frequency; LMD$_{High}$, mean deviations for L-cones at high frequency; SMD, S-cones at low frequency; RMD, rods at intermediate frequencies.

connected to facilitate intraindividual comparison, so that large differences are highlighted by steep slopes.

For the patients with FF, the MDs were normal for all photoreceptor subtypes, but there was a tendency toward rod dysfunction in Patient 3. Two out of three patients with BEM and all of the patients with CFA had reduced MD values, except for Patient 5, who had a positive LMD$_{Low}$. There was a tendency toward lower LMD$_{High}$ values.

Patient 9 had an extremely low LMD$_{Low}$ value and a not-measurable LMD$_{High}$ value, likely due to protanopy. This patient had CFA, but her data cannot be directly compared with the other patients from this group, so we show her data in a separate panel in Figure 6.

The mean deviations of the patients with STGD1/FF indicate significant sensitivity losses compared with normal subjects (LMD$_{low}$, $P = 0.016$; LMD$_{high}$, $P = 0.002$; RMD, $P = 0.004$). SMD nearly reached statistical significance ($P = 0.057$).

A Kruskall–Wallis test that was performed across all patient groups revealed no differences between the different photoreceptor classes ($P = 0.366$; eta2[H] = 0.0033). However, when we compared the differences among the FF, BEM, and CFA groups, the LMD$_{high}$ values were significantly different among the classification groups ($P = 0.045$; eta2[H] = 0.38). A post hoc Dunn's test indicated a statistical difference between the CFA and FF groups ($P = 0.016$) (Table 5).

Correlations among photoreceptor-/pathway-specific MDs are displayed in Figure 7. LMD$_{high}$ was strongly correlated with LMD$_{Low}$ ($t = 3.7219$; $P = 0.0034$; $R = 0.7465$), SMD ($t = 3.2082$; $P = 0.0094$; $R = 0.7121$), and RMD ($t = 2.3173$; $P = 0.0491$; $R = 0.63$). LMD$_{Low}$ was correlated with RMD ($t = 2.8263$; $P = 0.0223$; $R = 0.71$) and with SMD ($t = 2.5511$; $P = 0.0269$; $R = 0.61$), but there were no correlations between RMD and SMD.

Relationship Between tCS Mean Deviation and Clinical Parameters

LogMAR best-corrected visual acuity was the only parameter that significantly differed between diagnosis groups (Kruskall–Wallis, $P = 0.016$; eta2[H] = 0.56), in contrast to IR-SLO AoH or perimetric MD$_{6deg}$. A post hoc Dunn's test indicated that these differences were most pronounced between the BEM and CFA groups ($P = 0.034$), with the CFA
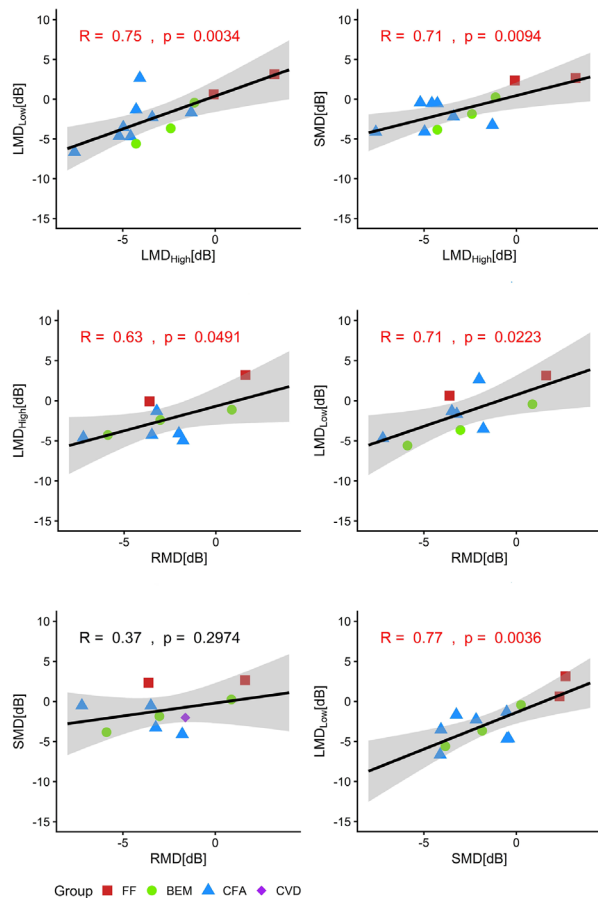
TABLE 5. Comparison by Group, with Medians (First; Third Quartiles) for Continuous Variables and n (%) for Subject Gender

Variable	BEM ($n = 3$)	CFA ($n = 8$)	FF ($n = 2$)	Overall P
Age	34.0 (32.0; 37.0)	43.5 (30.0; 61.2)	54.0 (54.0; 54.0)	0.443
Female gender	1 (33.3)	4 (50.0)	0 (0.00)	—
LogMAR	0.03 (0.01; 0.06)	0.79 (0.51; 0.90)	0.32 (0.24; 0.41)	0.016*
AoH	5.29 (4.34; 6.64)	4.76 (3.92; 6.28)	0.00 (0.00; 0.00)	0.098
MD_{12}	−8.41 (−12.00; −5.54)	−10.52 (−13.58; −9.84)	−1.94 (−2.59; −1.29)	0.196
LMD_{Low}	−3.66 (−4.63; −2.05)	−2.89 (−4.65; −1.58)	1.88 (1.25; 2.51)	0.139
LMD_{High}	−2.40 (−3.34; −1.76)	−4.43 (−5.03; −3.91)	1.56 (0.74; 2.38)	0.045*
SMD	−1.85 (−2.84; −0.80)	−2.18 (−3.66; −0.52)	2.50 (2.42; 2.58)	0.089
RMD	−3.02 (−4.46; −1.08)	−3.22 (−3.49; −2.01)	−1.00 (−2.31; 0.31)	0.834

Patient 9 was found to be protanopic, and her LMD data were excluded from analysis.
* Significant results.

FIGURE 7. Correlation among sensitivity deviations in the different photoreceptor types. CVD, color vision defect (Patient 9, whose data were not included in correlations with LMD).

DISCUSSION

Temporal contrast sensitivity was reduced in most patients, and there was no clear indication of selective damage in any photoreceptor type and/or post-receptoral pathway. TCSs were near normal in patients with FF. Luminance-driven tCS deviations (i.e., L-cone MDs at high frequencies) were significantly different among patient groups (FF vs. CFA), and they were also correlated with AoH and with MD_{6deg}.

Measuring Temporal Contrast Sensitivity in Patients With STGD1/FF

Visual function in STGD1/FF is usually characterized using best-corrected visual acuity and microperimetry ("standard of care"). Temporal contrast sensitivity has been used in experimental settings in order to investigate photoreceptor function. In studies based on increment thresholds,[33] critical flicker fusion frequency,[34] and rod thresholds,[34] retinal function was often only slightly reduced. Seiple et al.,[35] who analyzed tCS functions measured by Kayazawa et al.,[36] found greater tCS losses at intermediate than at higher temporal frequencies and considered this to be evidence for altered temporal processing in damaged but viable photoreceptors.

However, recent studies have obtained evidence that, even in diseases of the outer retina, psychophysical thresholds cannot be interpreted purely in terms of photoreceptors. White-on-white perimetric stimuli are usually detected by the luminance pathways,[37] but Simunovic et al.[15] demonstrated that this is not always the case for chromatic stimuli and that the mechanism mediating perception may depend on eccentricity.

Furthermore, Jolly et al.[38] found that remodeling of the inner retina, as demonstrated with measures of inner retinal thickness, affected microperimetric thresholds in patients with the *RPGR* gene. Our study gives no clear functional indication for remodeling in patients with STGD1/FF, supporting the validity of microperimetry as a functional biomarker in STGD1/FF.

Patient 9's low sensitivity for M-cone stimuli at low temporal frequencies (see Fig. 4, second panel from the top) highlights both the importance of postreceptoral mechanisms in photoreceptor diseases and the interaction between photoreceptors and postreceptoral pathways. In addition to having STGD1/FF, this female patient seemed to be protanope, as she was unable to detect L-cone–isolating stimuli and had typical sequence variants in the opsin genes. At high frequencies, M-cone function was normal, indi-
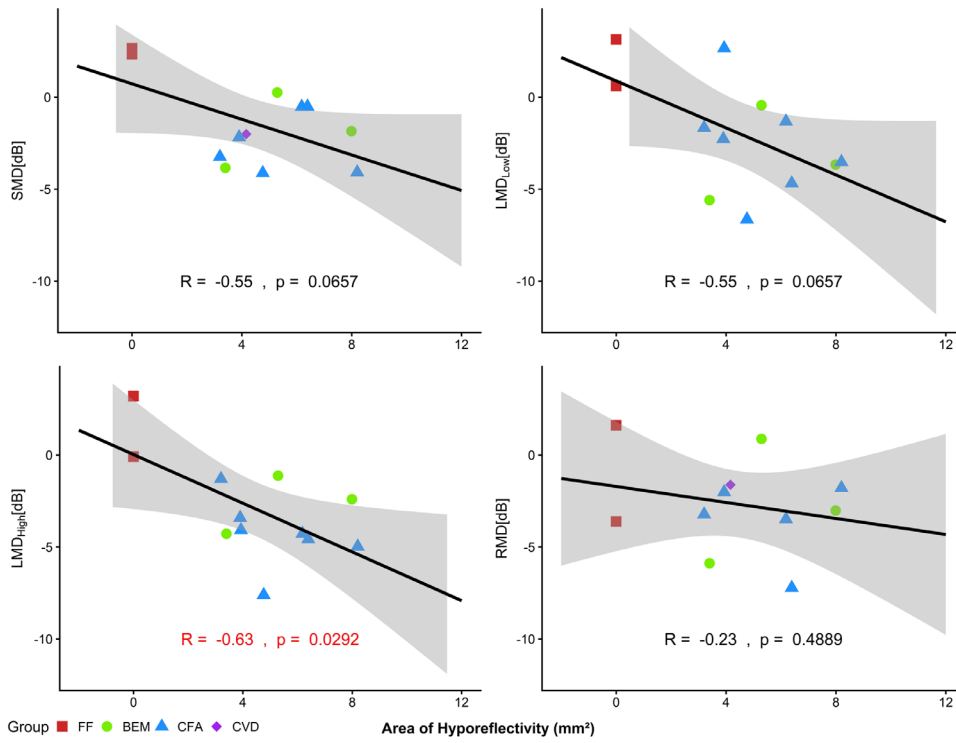
group having lower logMAR values. There was no correlation among these three clinical parameters (data not shown).

The defect size in the infrared scan AoH (Fig. 8) was not correlated with RMD, but was correlated with LMD_{High} ($t = −2.7191$; $P = 0.0263$; coefficient = −0.69).

The perimetric MD_{6deg} (Fig. 9) was correlated with LMD_{High} ($t = 3.4331$; $P = 0,0066$; $R = 0,74$) but also with LMD_{Low} ($t = 2.3671$; $P = 0.0395$; $R = 0.60$) and with SMD ($t = 2.6718$; $P = 0.0234$; $R = 0.65$).

FIGURE 8. Correlations among the contrast sensitivity deviations in the different photoreceptor subtypes and the AoH. CVD, color vision defect (Patient 9, whose data were used only for SMD and RMD).
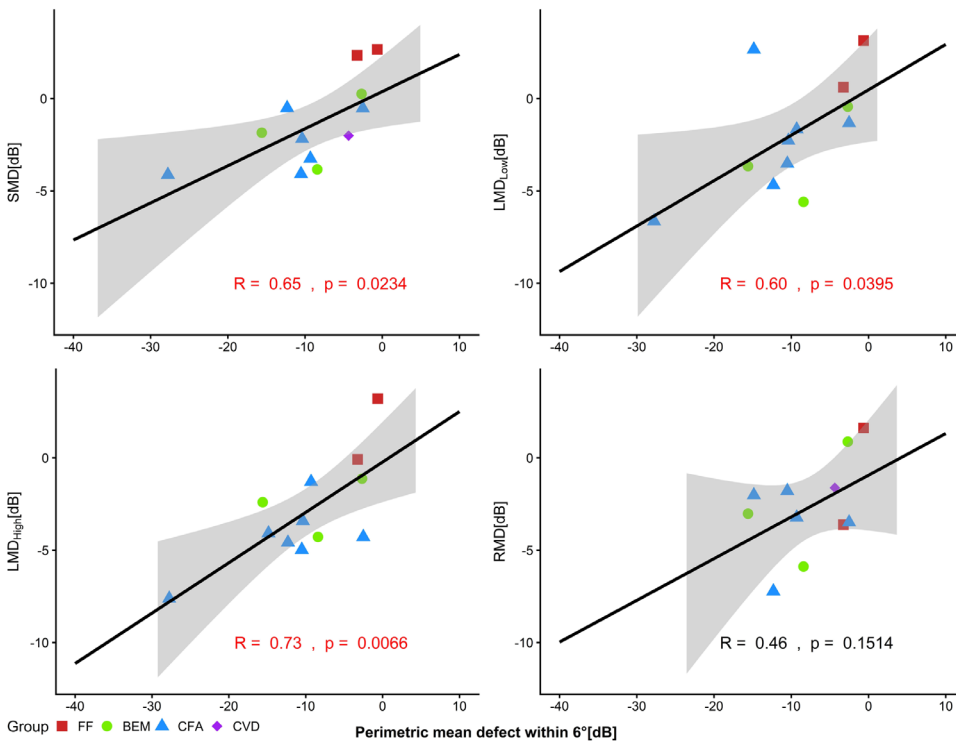

FIGURE 9. Correlations among the contrast sensitivity deviations in the different photoreceptor subtypes and the MD_{6deg} (standard automated perimetry). CVD, color vision defect (Patient 9, whose data were used only for SMD and RMD).

cating normal M-cones. Thus, the absence of a red–green opponency mechanism is most probably the reason for the reduction of M-cone–driven tCS at low frequencies—exceeding those in the other STGD patients—rather than an M-cone loss per se (L-cone stimuli are detected by the color system at low temporal frequencies and by the luminance system at high temporal frequencies, even when stimuli have more luminance contrast than color contrast[23]).

In age-related macular degeneration, loss of rod function has already been established as an early biomarker.[39] For STGD1/FF, several authors have suggested that dark-adapted, rod-mediated microperimetry can detect loss of retinal function earlier, as well.[13,14] Initially, *ABCA4* was thought to be expressed in rods only,[1] but Molday et al.[2] demonstrated that *ABCA4* is also expressed in cones. Reduced scotopic function has been well established in STGD1/FF (prolonged rod recovery[40] in dark adaptation, loss of scotopic function in ERG[11,41]). Using static two-color perimetry, Gerth et al.[42] also observed reduced rod function in some patients, but this did not correlate to other clinical or genetic observations.

The results of our study do not support the notion of more pronounced functional loss in rod-driven sensitivity, probably because our technique differed in two ways. First, we measured rod function at relatively high, mesopic light levels, which is possible with the silent substitution technique.[19,21] This allowed us to avoid prolonged dark adaptation and greatly simplified measurements. In this case, flicker perception was conveyed by the fast rod pathway via gap junctions between rods and cones and not by the slow pathway via rod bipolar cells. Possibly, early detection of photoreceptor loss is facilitated by reduced redundancy when tapping the slow rod–bipolar pathway.[43] Second, we measured rods and cones with identical retinal adaptation, and asymmetrical adaptation can also explain seemingly predominant loss of rod function.[44] In fact, Collison et al.[45] found that, when both rods and cones were measured at absolute threshold, cone function losses even exceeded rod function losses.

Feigl et al.[46] used an LED stimulator identical to ours for creating both pure cone-mediated and combined cone- and rod-mediated luminance signals. They found that mesopic critical fusion frequencies for combined cone and rod stimuli were reduced in persons with genetic risk factors for age-related macular degeneration (but with a normal fundus). This was not the case for pure cone stimuli. Therefore, an alternative explanation for the lack of a predominance of rod over cone dysfunction in our experiments may be that preferred rod damage occurs only in early stages of retinal degeneration in morphologically almost normal retina. In contrast to our measurements with a large stimulus, such changes might be detected in perimetric measurements even in the presence of areas of retinal atrophy. There was a slight tendency for decreased rod function in the two FF patients, but the size of our cohort is much too small for firm conclusions.

Relationship Between Clinical Parameters and tCS

tCS was not correlated with logMAR because many patients had preserved foveal function. It has been shown that logMAR is not well suited for detecting progression in STGD1/FF.[9,47] The LMD_{High} values were significantly lower in the CFA group. Also, LMD_{High} was significantly correlated with both MD_{6deg} and with the AoH on IR-SLO. We used IR-SLO instead of fundus autofluorescence because the AoH corresponds better with the area of reduced sensitivity in microperimetry.[48] Both standard automated perimetry and LMD_{High} are mediated by the magnocellular pathway, which is dominated by L-cones in the central retina.[37] Altogether, our results show that L-cone sensitivity at high frequencies is best suited for investigating structure–function relationships and corresponds best to perimetry.

Limitations

A limitation of our study is the small sample size of patients with STGD1/FF, the high prevalence of very mild phenotypes, and the absence of end-stage disease.

Eccentric fixation is a relevant challenge, as an earlier study on functional tests in patients with STGD1/FF did show.[32] Jackson et al.[49] observed that patients with STGD1/FF may adjust fixation, when instructed properly. We instructed patients to fixate so that they saw an annular stimulus and that their scotoma was in the center of the test field, and most patients reported to be able to do so. Thus, although we were not able to monitor either fixation locus or fixation stability with our setup, this approach must have minimized the effects of unstable eccentric fixation.

When using the silent substitution technique, the presence of X-linked color vision defects must be excluded, because the calculation of the tCS is based on the spectral sensitivities of normal photoreceptors. However, our data show that identification of patients with concomitant color vision defects is possible from the tCS curves. Indeed, we identified protanopy in one patient (Patient 9). Minor congenital deuteranomalies or protanomalies are less easy to detect with color vision tests, because patients with STGD1 have acquired color vision deficits (mostly pseudo-protanomaly[50]) and because tests such as the Panel D15 have a suboptimal sensitivity for small defects.[51] In contrast to dichromats,[18] detecting anomalous trichromats with the tCS curves is probably also more difficult. This issue can be addressed in the future by sequencing *OPN1LW* and *OPN1MW* genes.

Restricted spatial resolution can be considered another limitation of our technique, because very localized changes in retinal function may not be detected. Finally, we cannot draw conclusions from this cross-sectional study about the value of measuring photoreceptor-specific tCSs in longitudinal studies. We are currently conducting a study of longitudinal change of photoreceptor-specific tCS.

Implications

Photoreceptor-specific temporal contrast sensitivities can be used to quantify visual function in patients with STGD1/FF, making it a potential outcome parameter for clinical trials. This would necessitate simplification of the testing protocol and a different apparatus, possibly based on video projectors. Our technique enables controlling the post-receptoral pathways that mediate detection, and it also allows measuring rod function at relatively high mesopic light levels.

CONCLUSIONS

Temporal contrast sensitivity is a potential biomarker for photoreceptor-specific function loss in the perifovea in

STGD1/FF. Although we did not find selective damage in any specific photoreceptor class or post-receptoral mechanism, luminance-driven L-cone–isolating temporal contrast sensitivities are a potential parameter for visual function in clinical studies.

References

1. Allikmets R, Singh N, Sun H, et al. A photoreceptor cell-specific ATP-binding transporter gene (*ABCR*) is mutated in recessive Stargardt macular dystrophy. *Nat Genet*. 1997;15(3):236–246.

2. Molday LL, Rabin AR, Molday RS. ABCR expression in foveal cone photoreceptors and its role in Stargardt macular dystrophy. *Nat Genet*. 2000;25(3):257–258.

3. Stargardt K. Ueber die familiaere, progressive Degeneration in der Makulagegend des Auges. *Graefes Arch Clin Exp Ophthalmol*. 1909;71:534–550.

4. Fujinami K, Sergouniotis PI, Davidson AE, et al. Clinical and molecular analysis of Stargardt disease with preserved foveal structure and function. *Am J Ophthalmol*. 2013;156(3):487–501.e1.

5. Fishman GA. Fundus flavimaculatus. A clinical classification. *Arch Ophthalmol*. 1976;94(12):2061–2067.

6. Cremers FP, van de Pol DJ, van Driel M, et al. Autosomal recessive retinitis pigmentosa and cone-rod dystrophy caused by splice site mutations in the Stargardt's disease gene *ABCR*. *Hum Mol Genet*. 1998;7(3):355–362.

7. Martínez-Mir A, Paloma E, Allikmets R, et al. Retinitis pigmentosa caused by a homozygous mutation in the Stargardt disease gene *ABCR*. *Nat Genet*. 1998;18(1):11–12.

8. Salvatore S, Fishman GA, McAnany JJ, Genead MA. Association of dark-adapted visual function with retinal structural changes in patients with Stargardt disease. *Retina*. 2014;34(5):989–995.

9. Rotenstreich Y, Fishman GA, Anderson RJ. Visual acuity loss and clinical observations in a large series of patients with Stargardt disease. *Ophthalmology*. 2003;110(6):1151–1158.

10. Fishman GA, Stone EM, Grover S, Derlacki DJ, Haines HL, Hockey RR. Variation of clinical expression in patients with Stargardt dystrophy and sequence variations in the *ABCR* gene. *Arch Ophthalmol*. 1999;117(4):504–510.

11. Moloney JB, Mooney DJ, O'Connor MA. Retinal function in Stargardt's disease and fundus flavimaculatus. *Am J Ophthalmol*. 1983;96(1):57–65.

12. Schneider T, Zrenner E. Rod-cone interaction in patients with fundus flavimaculatus. *Br J Ophthalmol*. 1987;71(10):762–765.

13. Cideciyan AV, Swider M, Aleman TS, et al. ABCA4 disease progression and a proposed strategy for gene therapy. *Hum Mol Genet*. 2009;18(5):931–941.

14. Strauss RW, Kong X, Bittencourt MG, et al. Scotopic Microperimetric Assessment of Rod Function in Stargardt Disease (SMART) study: design and baseline characteristics (report no. 1). *Ophthalmic Res*. 2019;61(1):36–43.

15. Simunovic MP, Moore AT, MacLaren RE. Selective automated perimetry under photopic, mesopic, and scotopic conditions: detection mechanisms and testing strategies. *Transl Vis Sci Technol*. 2016;5(3):10.

16. Donner KO, Rushton WA. Retinal stimulation by light substitution. *J Physiol*. 1959;149(2):288–302.

17. Estevez O, Spekreijse H. The "silent substitution" method in visual research. *Vision Res*. 1982;22(6):681–691.

18. Huchzermeyer C, Kremers J. Perifoveal L- and M-cone-driven temporal contrast sensitivities at different retinal illuminances. *J Opt Soc Am A Opt Image Sci Vis*. 2016;33(10):1989–1998.

19. Huchzermeyer C, Kremers J. Perifoveal S-cone and rod-driven temporal contrast sensitivities at different retinal illuminances. *J Opt Soc Am A Opt Image Sci Vis*. 2017;34(2):171–183.

20. Huchzermeyer C, Fars J, Kremers J. Photoreceptor-specific loss of perifoveal temporal contrast sensitivity in retinitis pigmentosa. *Transl Vis Sci Technol*. 2020;9(6):27.

21. Maguire J, Parry NRA, Kremers J, Kommanapalli D, Murray IJ, McKeefry DJ. Rod electroretinograms elicited by silent substitution stimuli from the light-adapted human eye. *Transl Vis Sci Technol*. 2016;5(4):13.

22. Aher AJ, McKeefry DJ, Parry NRA, et al. Rod- versus cone-driven ERGs at different stimulus sizes in normal subjects and retinitis pigmentosa patients. *Doc Ophthalmol*. 2018;136(1):27–43.

23. Huchzermeyer C, Horn F, Lämmer R, Mardin C, Kremers J. Summation of temporal L-cone- and M-cone-contrast in the magno- and parvocellular retino-geniculate systems in glaucoma. *Invest Ophthalmol Vis Sci*. 2021;62(6):17.

24. Pokorny J, Smithson H, Quinlan J. Photostimulator allowing independent control of rods and the three cone types. *Vis Neurosci*. 2004;21(3):263–267.

25. Puts MJH, Pokorny J, Quinlan J, Glennie L. Audiophile hardware in vision science; the soundcard as a digital to analog converter. *J Neurosci Methods*. 2005;142(1):77–81.

26. Shapiro AG, Pokorny J, Smith VC. Cone-rod receptor spaces with illustrations that use CRT phosphor and light-emitting-diode spectra. *J Opt Soc Am A Opt Image Sci Vis*. 1996;13(12):2319–2328.

27. Stockman A, Sharpe LT. The spectral sensitivities of the middle- and long-wavelength-sensitive cones derived from measurements in observers of known genotype. *Vision Res*. 2000;40(13):1711–1737.

28. Stockman A, Sharpe LT, Fach C. The spectral sensitivity of the human short-wavelength sensitive cones derived from thresholds and color matches. *Vision Res*. 1999;39(17):2901–2927.

29. Wald G. Human vision and the spectrum. *Science*. 1945;101(2635):653–658.

30. Marín-Franch I, Swanson WH. The visualFields package: a tool for analysis and visualization of visual fields. *J Vis*. 2013;13(4):10.

31. Smith VC, Pokorny J, Davis M, Yeh T. Mechanisms subserving temporal modulation sensitivity in silent-cone substitution. *J Opt Soc Am A Opt Image Sci Vis*. 1995;12(2):241–249.

32. Messias A, Reinhard J, e Cruz AAV, Dietz K, MacKeben M, Trauzettel-Klosinski S. Eccentric fixation in Stargardt's disease assessed by Tübingen perimetry. *Invest Ophthalmol Vis Sci*. 2007;48(12):5815–5822.

33. Zrenner E, Nowicki J, Adamczyk R. Cone function and cone interaction in hereditary degenerations of the central retina. *Doc Ophthalmol*. 1986;62(1):5–12.

34. Itabashi R, Katsumi O, Mehta MC, Wajima R, Tamai M, Hirose T. Stargardt's disease/fundus flavimaculatus: psychophysical and electrophysiologic results. *Graefes Arch Clin Exp Ophthalmol*. 1993;231(10):555–562.

35. Seiple W, Greenstein V, Carr R. Losses of temporal modulation sensitivity in retinal degenerations. *Br J Ophthalmol.* 1989;73(6):440–447.

36. Kayazawa F, Sonoda K, Nishimura K, Nakamura T, Yamamoto T, Itoi M. Clinical application of temporal modulation transfer function. *Jpn J Ophthalmol.* 1984;28(1):9–19.

37. Swanson WH, Sun H, Lee BB, Cao D. Responses of primate retinal ganglion cells to perimetric stimuli. *Invest Ophthalmol Vis Sci.* 2011;52(2):764–771.

38. Jolly JK, Menghini M, Johal PA, Buckley TMW, Bridge H, Maclaren RE. Inner retinal thickening affects microperimetry thresholds in the presence of photoreceptor thinning in patients with RPGR retinitis pigmentosa [published online ahead of print October 30, 2020]. *Br J Ophthalmol*, https://doi.org/10.1136/bjophthalmol-2020-317692.

39. Owsley C, McGwin G, Clark ME, et al. Delayed rod-mediated dark adaptation is a functional biomarker for incident early age-related macular degeneration. *Ophthalmology.* 2015;123(2):344–351.

40. Fishman GA, Farbman JS, Alexander KR. Delayed rod dark adaptation in patients with Stargardt's disease. *Ophthalmology.* 1991;98(6):957–962.

41. Lois N, Holder GE, Bunce C, Fitzke FW, Bird AC. Phenotypic subtypes of Stargardt macular dystrophy-fundus flavimaculatus. *Arch Ophthalmol.* 2001;119(3):359–369.

42. Gerth C, Andrassi-Darida M, Bock M, Preising MN, Weber BH, Lorenz B. Phenotypes of 16 Stargardt macular dystrophy/fundus flavimaculatus patients with known ABCA4 mutations and evaluation of genotype–phenotype correlation. *Graefes Arch Clin Exp Ophthalmol.* 2002;240(8):628–638.

43. Sharpe LT, Stockman A, MacLeod DI. Rod flicker perception: scotopic duality, phase lags and destructive interference. *Vision Res.* 1989;29(11):1539–1559.

44. Simunovic MP, Hess K, Avery N, Mammo Z. Threshold versus intensity functions in two-colour automated perimetry. *Ophthalmic Physiol Opt.* 2021;41(1):157–164.

45. Collison FT, Fishman GA, McAnany JJ, Zernant J, Allikmets R. Psychophysical measurement of rod and cone thresholds in Stargardt disease with full-field stimuli. *Retina.* 2014;34(9):1888–1895.

46. Feigl B, Cao D, Morris CP, Zele AJ. Persons with age-related maculopathy risk genotypes and clinically normal eyes have reduced mesopic vision. *Invest Ophthalmol Vis Sci.* 2011;52(2):1145–1150.

47. Kong X, Fujinami K, Strauss RW, et al. Visual acuity change over 24 months and its association with foveal phenotype and genotype in individuals with Stargardt disease: ProgStar Study report no. 10. *JAMA Ophthalmol.* 2018;136(8):920–928.

48. Anastasakis A, Fishman GA, Lindeman M, Genead MA, Zhou W. Infrared scanning laser ophthalmoscope imaging of the macula and its correlation with functional loss and structural changes in patients with Stargardt disease. *Retina.* 2011;31(5):949–958.

49. Jackson ML, Seiple W. Stargardt macular dystrophy: changes in fixation when asked to look straight ahead. *Ophthalmol Retina.* 2017;1(6):524–530.

50. Pokorny J, Smith VC, Ernest JT. Macular color vision defects: specialized psychophysical testing in acquired and hereditary chorioretinal diseases. *Int Ophthalmol Clin.* 1980;20(1):53–81.

51. Huchzermeyer C, Kremers J, Barbur J. Color vision in clinical practice. In: Kremers J, Baraas RC, Marshall NJ , eds. *Human Color Vision.* New York: Springer International; 2016:269–315.